PAPR and BER Performance Analysis of OFDM System with Multi-h CPFSK Mapper

Emammer Shafter, Abdulbaset M. Hamed, and Raveendra K. Rao
Faculty of Engineering, Department of Electrical and Computer Engineering
University of Western Ontario, London, Ontario, N6A 5B9. Canada
Email: {eshafter, ahamed6, rrao}@uwo.ca

***Abstract*—Multi-h CPFSK mapper in an OFDM system can offer significant gain in both PAPR and bit error rate probability. The OFDM PAPR problem is addressed and investigated using SLM reduction technique. Next, an OFDM system with a multi-h CPFSK mapper is considered and its performance is evaluated in terms of the upper and lower bounds on bit error rate probability, and a closed form expression is obtained. Also, the system performance is examined over Rayleigh and Nakagami-m fading channels. The simulation and analytical results show that the performance of the system is superior than the OFDM system with BPSK and single-h CPFSK mappers.**

***Keywords*—OFDM, Multi-h CPFSK, PAPR, SLM, Rayleigh, Nakagami-m**

I. INTRODUCTION

The OFDM system is being widely used in several communication standards due to its spectral efficiency and cost effectiveness. Several mappers have been used in OFDM systems such as QAM, PSK, and DPSK, and their performance have been investigated for different fading channels [1] and [2]. The CPM is a non-linear digital modulation technique which provides significant trade-offs among bandwidth, power, and complexity of communication systems due to its constant envelope. Continuous-phase frequency shift keying (CPFSK) is a special case of CPM, where the phase changes linearly with time. In [3], the performance of binary single-h CPFSK was examined for AWGN, Rayleigh, Nakagami-m, and Generalized-K channels in terms of the system modulation index and observation interval. Multi-h CPFSK provides a robust performance, as analyzed in [4]. Thompson *et al.* [5] have introduced the notion of constant envelop OFDM system, and its performance has been investigated for AWGN and fading channels. Also in [6], the PAPR reduction technique using SLM for the single-h CPFSK OFDM system was addressed and analyzed. To the best of our knowledge, the bit error rate performance of multi-h CPFSK OFDM system over multi-path fading channels has not been investigated. The intent of this paper is to introduce a multi-h CPFSK mapper with memory in an OFDM system for two purposes: i) reduce PAPR of the transmitted OFDM signal; and ii) enhance the bit error probability performance of the system. In particular, the PAPR of multi-h CPFSK OFDM with SLM reduction technique is examined, and the receiver performance of the system is analyzed over Rayleigh and Nakagami-m channels. The remainder of this paper is organized as follows: Section II describes multi-h CPFSK mapper in an OFDM transmitter. The PAPR of the system using SLM reduction technique is presented and evaluated in Section III. The upper and lower bound of the bit error rate performance of the system in AWGN are obtained in Section IV. The lower bound is also derived for multi-path fading channels. In Section V, the simulation and analytical results are provided with discussion. Finally, the paper is concluded in Section VI.

II. SYSTEM MODEL

The block diagram of the OFDM system with a multi-h CPFSK mapper is shown in Fig.1. The system consists of N multi-carrier modulator and multi-h CPFSK mapper at the transmitter side. The wireless channel is represented by a multi-path fading and AWGN. The receiver includes a multi carrier demodulator and multi-h CPFSK demapper. The input data stream is grouped into N sub-blocks data, with a length of Z by the S/P block. The data is expressed by the matrix $\vec{\mathbf{a}}_{T_{N\times Z}}$, and its elements are $a_{u,v} = \pm 1$ for the CPFSK binary case where $u = 1, , 2, ..., N$ and $v = 1, , 2, ..., Z$. The data matrix $\vec{\mathbf{a}}_{T_{N\times Z}}$ is then fed to the CPFSK mapper, and it produces symbols with phases according to the data sequence, which is represented by the matrix $\vec{C}_{T_{N\times Z}}$. As shown in Fig.1, the input data is fed

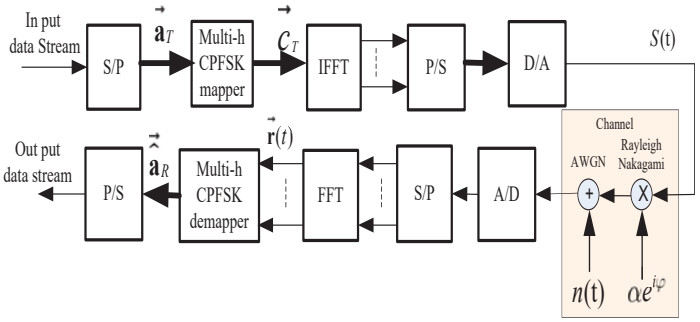

Fig. 1: General block diagram of multi-h CPFSK OFDM system

to the CPFSK mapper before the OFDM system. The mapper converts the data matrix , $\vec{\mathbf{a}}_{T_{N\times Z}}$, to appropriate a complex $N \times Z$ matrix, $\vec{\mathbf{C}}_{T_{N\times Z}}$, with elements as

$$c_{u,v} = \cos(\theta_{u,v}) + j\sin(\theta_{u,v})$$

$$\theta_{u,v} = a_{u,v}\pi h + \pi h \sum_{q=0}^{u-1} a_{q,v} + \phi \qquad (1)$$

The multi-h CPFSK mapper varies the parameter h for each data input $a_{u,v}$, where the h is cyclically chosen from the set $\{h_1, h_2, ..., h_K\}$. For an illustration, we take the first four symbols for an arbitrary u^{th} sub-carrier with $h = \{3/4, 2/3\}$ and data sequence $a_{u,v} = [+1, +1, -1, +1]$. Assuming the initial phase is set to be zero, then the number of possible phase states, $\theta_{u,v}$ for $h = 3/4$ and $2/3$ would be 4 and 3, respectively. The output signal of the OFDM transmitter is then represented as

$$S(t) = \sum_{u=1}^{N}\sum_{v=1}^{Z} c_{u,v} e^{j\frac{2\pi}{NT_b}vt}, \quad 0 \le t < \infty \qquad (2)$$

where T_b is the bit duration.

III. OFDM PAPR Problem Formulation

The major drawback of the OFDM system is that the sub-carriers have a non-constant envelop with high peaks, that causes the instantaneous power to be higher than the average power. In this paper, the SLM technique is employed to minimize the PAPR of the proposed OFDM system. The SLM technique is based on generating Q permutations OFDM symbols $\overrightarrow{C}_T$ each of length Z, which carries the same information as the original signal, then transmits the one with the minimum PAPR for each row of the symbol matrix $\overrightarrow{C}_{T_{N\times Z}}$ as shown in Fig.2. The Q data blocks are multiplied by a phase vector $\vec{B}_u = [b_{u,1}, b_{u,2}, ..., b_{u,Q}]^T$, and $b_{u,1} = [e^{\phi_{1,1}}, e^{\phi_{1,2}}, ..., e^{\phi_{1,Z}}]$, which produces the vector $\overrightarrow{\hat{C}}_{T_{N\times Z}} = [\hat{C}_1 b_{u,1}, \hat{C}_2 b_{u,2}, ..., \hat{C}_Z b_{u,Z}]^T$, and is then applied to the IFFT. From the output of the IFFT, the one with the lowest PAPR is selected for transmission and inset to the $\widehat{S}(t) = [\hat{S}_1, \hat{S}_2, ..., \hat{S}_N]^T$ signal output vector.

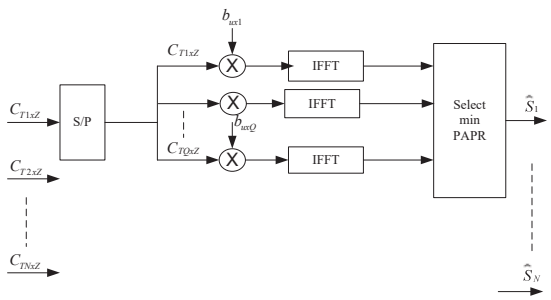

Fig. 2: A block diagram of OFDM with SLM PAPR reduction technique

The complex baseband signal of the OFDM system without the PAPR reduction technique can be written as:

$$S(t) = \frac{1}{\sqrt{N}} \sum_{u=1}^{N} C_u \ \exp^{j2\pi u \triangle f t}, \qquad 0 \le t < NT_b, \tag{3}$$

where $\Delta f (= 1/NT_b)$ is the sub-carrier spacing, NT_b is the data block period, and N is the number of sub-carriers in the system. The PAPR of the OFDM is defined as the ratio between the maximum instantaneous power to the average power, given by:

$$PAPR = \frac{max|S(t)|^2}{\frac{1}{NT}\int_0^{NT} |S(t)|^2 dt}, \quad 0 \ \le \ t \ \le \ NT \tag{4}$$

In the computation of PAPR, NL equidistant samples of $S(t)$ is considered, where L is an integer and greater than or equal to 1. These L-times oversampled signal samples are represented as a vector $\overrightarrow{S_T} = [S_1, S_2, ..., S_{NL}]^T$, and each element is represented by

$$S_k = \frac{1}{\sqrt{N}} \sum_{u=1}^{N} C_u \ \exp^{j2\pi k u \Delta f T/L}, \ k = 1, 2, ...NL \tag{5}$$

It is noted that the sequence S_k can be interpreted as the inverse fast Fourier transform IFFT of data block C with $(L-1)N$ zero padding. In fact, for an accurate measure of the PAPR, the signal is sampled with $L = 4$. Thus, PAPR can be defined as

$$PAPR = \frac{max|S_k|^2}{E[|S_k|^2]}, \ 0 \ \le \ k \ \le \ LN - 1 \tag{6}$$

where E[.] is the average signal power. The sampling rate is the Nyquist rate or a multiple of it. It has been proved that using an oversampling of $L = 4$ results in discrete time PAPR that closely matches continuous time [6]. The output of the IFFT block for this modified data with an oversampling factor of L is given by

$$S_k^{(u)} = \frac{1}{\sqrt{N}} \sum_{u=1}^{N} C_u b_u \ e^{j2\pi k u \Delta f T/L}, \tag{7}$$

The PAPR for each $\{S_k^{(u)}, k = 1, 2, ..., NL\}, u = 1, 2, ..., N$, block is computed and then the minimum of these is chosen for transmission. That is,

$$\min_{1\le u\le U} \{S_k^{(u)}, k = 1, 2, ..., NL\} \tag{8}$$

The generated phase matrix $\vec{B}$ has to be transmitted to the receiver as side information, which reduces the system throughput.

IV. BER Performance

In this section, we evaluate the performance of the multi-h CPFSK demapper shown in Fig.1 in terms of bit error rate probability. The performance is investigated by first deriving the error probability bound expressions over AWGN and then over multi-path fading channels. Our analysis is based on the assumption that the $n_u(t), \ u = 1, 2, .., N$ is iid and $\sim \ \mathcal{N}(0, \ \sigma^2)$. Also, it is assumed that the fading channel is flat and non-selective fading, meaning all the sub-carriers experience the same amount of fading.

A. Upper and Lower Bounds of AWGN

The upper bound on error probability can be shown to be:

$$P_e = \frac{1}{K2^{n-1}} \sum_{l=1}^{2^n-1} \sum_{j=1}^{2^n-1} \sum_{p=1}^{K} Q\left(\sqrt{\frac{nE_b}{N_o}\left[1 - \rho_p\left(l, j\right)\right]}\right) \tag{9}$$

where $\rho_p(l, j)$ is the normalized correlation coefficient and can be derived using

$$\rho_p\left(l, j\right) = \frac{1}{nE_b} \int_0^{nT} S^{(p)}\left(t, -1, A_l\right) S^{(p)}\left(t, +1, A_j\right) dt \tag{10}$$

For multi-h CPFSK, the $\rho_p(l, j)$ is obtained as

$$\rho_p(l, j) = \text{Sinc}\left(\frac{1}{2} h_{[i]}^{(p)} \eta_i\right) \cos\left(\frac{\pi}{2} h_{[i]}^{(p)} \eta_i + \theta_i\right) \tag{11}$$

where $\theta_i = \pi \sum_{r=1}^{i-1} \eta_r h_{[r]}^{(p)}$ is the accumulated phase, $\eta_i = a_i^l - a_i^j$ is the difference sequence between data bits, taking values from the set $-2, \ 0, \ +2$. The cyclic arrangements of the K modulation indexes are given as $\{h_{[i]}^{(p)}; \ i = 1, ..., n\}, \ p = 1, ..., K$, for instance, $\{h_{[i]}^{(1)}\} = (h_1, ..., k_K, h_1, ...)$. The lower bound on probability of bit error can be obtained by assuming

that for each transmitted sequence, the demapper needs only decide between this sequence and its closest neighbor; this means $\rho_p(l) = \rho_p(l,j) \,|\max$ for all j^s. The expression for lower bound on probability bit error can then be written as

$$P_e = \frac{1}{K2^{n-1}} \sum_{l=1}^{2^{n-1}} \sum_{p=1}^{K} Q\left\{\sqrt{\frac{nE_b}{N_o}\left(1-\rho_p(l)\right)}\right\} \tag{12}$$

B. Performance over Fading Channel

The wireless communications environment is highly susceptible to the fading effect due to multi-path propagation. These effects cause major degradation in SNR, which impacts the system performance. Two models for small scale fading are considered in this work, specifically the Rayleigh and Nakagami-m distributions. In this work, the fading is assumed to be flat during the whole observation length (nT_b). The received OFDM signal with a multi-h CPFSK mapper over the fading channel can be expressed as

$$\vec{\mathbf{r}}(t) = \alpha \mathbf{S}(t) + \mathbf{n}(t) \tag{13}$$

The elements of $\vec{\mathbf{r}}(t)$ vector are $r_u = \alpha_u S_u(t) + n_u(t)$, where α_u is a random variable representing channel gain and $n_u(t)$ is the AWGN. For a multicarrier system, the instantaneous SNR and average SNR can be expressed as $\gamma_u = \alpha_u^2(\xi + E_b/N_o)$ and $\overline{\gamma_u} = \Omega_u(\xi + E_b/N_o)$ respectively. The ξ depends on the OFDM system parameters, such as the number of sub-carriers and pilot, and cyclic prefix where $\Omega_u = \overline{\alpha_u^2}$ for each u sub-carrier. The average bit error probability of multi-h CPFSK OFDM systems P_{av} over the fading channel is obtained by averaging the conditional error probability over the probability density function (pdf) of the fading model, given by [3]

$$P_{av} = \int_0^\infty P_e\left(\gamma_u|\alpha_u^2\right) f\left(\alpha_u^2\right) d\alpha_u \tag{14}$$

In our analysis, we consider Rayleigh and Nakagami-m channel models, which are commonly used in fading analyses.

1) Rayleigh Fading Channel: Rayleigh fading channel is a practicable model when there is no line-of-sight propagation between the transmitter and the receiver. In this case, $\alpha_u^2 \sim$ exp and its pdf is given [7]

$$f_R(\alpha_u) = \frac{1}{\Omega_u} \exp\left(-\frac{\alpha_u^2}{\Omega_u}\right), \quad \alpha_u \geq 0 \tag{15}$$

The average lower bound bit error probability over the Rayleigh fading channel can be derived by substituting (12) and (15) in (14). By expressing $Q(x) = \frac{1}{\pi}\int_0^{\frac{\pi}{2}} \exp\left(-\frac{x^2}{2\,sin^2(\theta)}\right) d\theta$, and with the aid of [8], the closed-form of P_{avR} is obtained as

$$P_{avR} = \frac{1}{NK2^n} \sum_{l=1}^{2^{n-1}} \sum_{p=1}^{K} \sum_{u=1}^{N} \left[1 - \sqrt{\frac{\overline{\gamma}_u \beta(l,n,p)}{\overline{\gamma}_u \beta(l,n,p)+1}}\right] \tag{16}$$

where $\beta(l,n,p) = \frac{n}{2}[1-\rho_p(l,n,p)]$.

2) Nakagami-m Fading Channel: In this section, we assume that $\alpha_u \sim$ Nakagami(m,Ω) which can model a variety of fading environments, such as Rayleigh for $m=1$, Rician for $m>1$, and AWGN when $m \to \infty$. $\alpha_u^2 \sim$ Gamma(m,Ω) and is given by [7]

$$f_N(\alpha_u) = \frac{2m^m \alpha_u^{2m-1}}{\Omega_u^m \Gamma(m)} \exp\left(-\frac{m\alpha_u^2}{\Omega_u}\right), \quad \alpha_u \geqslant 0 \tag{17}$$

The average lower bound bit error probability over the Nakagami-m fading channel can then be derived by using (12), (14) and (17). The introduced integration can be solved using [9, eq. (8.4.15/1),(2.24.1/1)] and the closed form is obtained as

$$P_{avN} = \frac{1}{NK2^n\sqrt{\pi}\Gamma(m)} \sum_{l=1}^{2^{n-1}} \sum_{p=1}^{K} \sum_{u=1}^{N} \times G_{2,2}^{2,1}\left(\beta(l,n,p)\frac{\overline{\gamma}_u}{m} \;\middle|\; \begin{matrix} 1,\ 1-m \\ 0,\ 1/2 \end{matrix}\right) \tag{18}$$

where $G_{q,p}^{a,b}\left(x \mid \begin{matrix}\cdots \\ \cdots\end{matrix}\right)$ is the Meijer G-function [9].

V. Numerical Results and Discussion

The two main performance metrics of the proposed OFDM system, which are PAPR and BER, are investigated. An intensive simulation is conducted for the multi-h CPFSK OFDM transmitter to measure the PAPR of the system output signal, (3), using (4). The simulation is done without the PAPR reduction technique, and then SLM is implemented in the system. The OFDM simulation parameters are given in Table.I. The obtained results are shown in Fig.3 for 128 sub-carriers, and a set of modulation indexes. For comparison purposes, the PAPR of the OFDM-BPSK system is also plotted. As can be seen, our introduced system, multi-h CPFSK OFDM, with SLM reduction technique, provides very low PAPR compared to the other

TABLE I: Simulation parameters

Symbol	Description	Value
N	Number of Sub-Carriers	128
h	Modulation index	$3/4, 2/3$
Q	Number of Sub-group	16
L	Oversampling factor	4
D	OFDM symbols	10^4

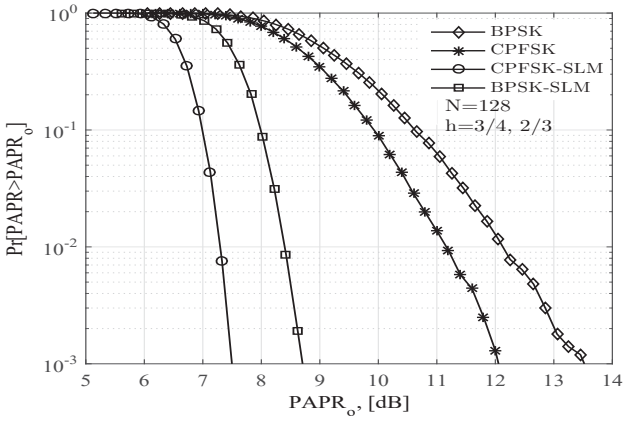

Fig. 3: PAPR Performance of 128 sub-carrier OFDM system multi-h CPFSK mapper

simulated systems. For instance, at probability of 10^{-3} the performance of the introduced system is superior to OFDM-BPSK, -CPFSK, and -BPSK-SLM with 6, 4.5, and 1.3 dB, which is a significant accomplishment. However, SLM increases the system complexity, and more details can be found in [10]. The system BER is evaluated in terms of the two bounds. The error probability of both upper and lower bounds are investigated as a function of signal-to-noise ratio SNR, observation intervals n, and a set of modulation indexes h_i. Fig.4 shows the plot of the upper and lower bounds for $h = 0.77, 0.62$ and $n = 2, 3$ as a function of E_b/N_o. The bit error rate for the OFDM-BPSK system is also plotted to show the performance improvement. It

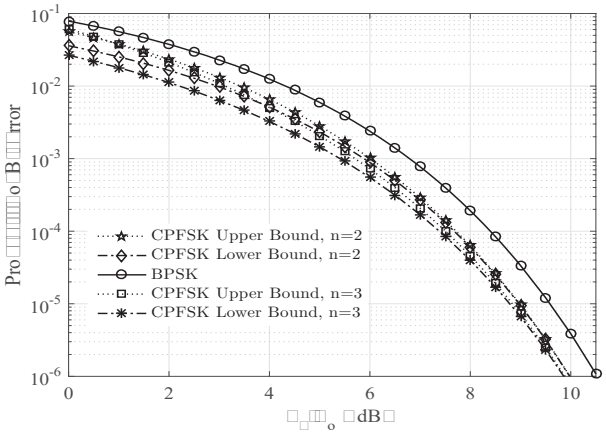

Fig. 4: BER performance of Multi-h CPFSK OFDM Systems Over AWGN for $n = 2, 3$

can be seen that the introduced multi-h CPFSK OFDM system performs better than the OFDM-BPSK by 1 dB on average. Also, it is noted that the bit error probability of $n = 3$ is slightly better than when $n = 2$; however, the receiver will be more complex as n increases. Our investigation includes the multi-path fading channel. The lower bound of the bit error probability over Rayleigh and Nakagami-m were derived in (16) and (18) for arbitrarily channel parameter (m), observation interval (n), modulation index (h), and number of OFDM sub-carriers. Since the fading channel is assumed to be flat and non-selective, and hence all OFDM sub-carriers are exposed to the same amount of fading, α_u is equivalent for all sub-carriers. The P_{avR} and P_{avN} are plotted in Fig.5 for $N = 128$, $m = 1,\ 3,\ 6,$ and $n = 2,\ 3$. The modulation index is set to $h = 0.77,\ 0.62$ which provides an optimal bit error probability. Fig.5 shows that the bounds of Nakagami-$m = 1$ and Rayleigh are matched that can be also mathematically proved by substituting $m = 1$ in (17) to yield (15) [11, eq.(07.34.03.0782.01)]. The bit error bound of Nakagami-m is improved as m increases, and it approaches AWGN for large values m.

VI. Conclusion

The OFDM with multi-h CPFSK mapper system has been introduced and then simulated to evaluate its performance. The SLM is proposed to reduce the PAPR of the OFDM system with multi-h CPFSK mapper. The PAPR was investigated for an arbitrary number of sub-carriers and modulation indexes. The performance of the multi-h CPFSK with coherent detection for

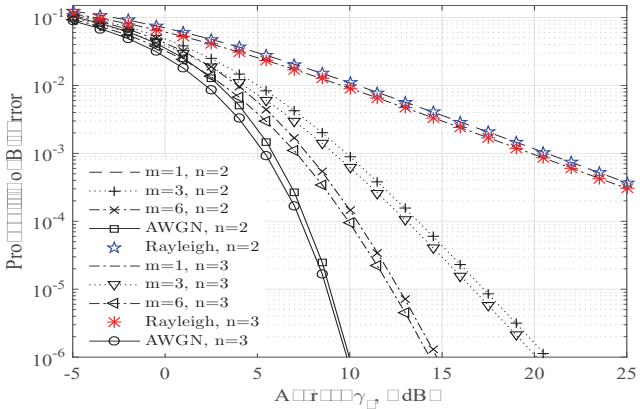

Fig. 5: BER performance of Multi-h CPFSK OFDM System Over Nakagami-m for $n = 2, 3$

the OFDM system is examined over Rayleigh, and Nakagami-m channels as a function of average SNR, observation interval, and modulation index. The introduced system achieves better performance than conventional OFDM systems.

References

[1] Yun Hee Kim, Iickho Song, Hong Gil Kim, Taejoo Chang and Hyung Myung Kim, "Performance analysis of a coded OFDM system in time-varying multipath Rayleigh fading channels," in IEEE Transactions on Vehicular Technology, vol. 48, no. 5, pp. 1610-1615, Sep 1999.

[2] Jun Lu, Tjeng Thiang Tjhung, F. Adachi and Cheng Li Huang, "BER performance of OFDM-MDPSK system in frequency-selective Rician fading with diversity reception," in IEEE Transactions on Vehicular Technology, vol. 49, no. 4, pp. 1216-1225, Jul 2000.

[3] A. M. Hamed, M. Alsharef and R. K. Rao, "Bit error probability performance bounds of CPFSK over fading channels," 2015 IEEE 28th Canadian Conference on Electrical and Computer Engineering (CCECE), Halifax, NS, 2015, pp. 1329-1334.

[4] K. R. Raveendra and R. Srinivasan, "Coherent detection of binary multi-h CPM," in Communications, Radar and Signal Processing, IEE Proceedings F, vol. 134, no. 4, pp. 416-426, July 1987.

[5] S. C. Thompson, A. U. Ahmed, J. G. Proakis, J. R. Zeidler and M. J. Geile, "Constant Envelope OFDM," in IEEE Transactions on Communications, vol. 56, no. 8, pp. 1300-1312, August 2008.

[6] E. Shafter and R. K. Rao, "CF technique with CPM mappers in OFDM systems for reduction of PAPR," 2016 IEEE Canadian Conference on Electrical and Computer Engineering (CCECE), Vancouver, BC, 2016, pp. 1-5.

[7] M. K. Simon and M.-S. Alouini, Digital Communication over Fading Channels, 2nd ed. New York: Wiley, 2005.

[8] I.S. Gradshteyn and I.M. Ryzhik, *Table of Integrals, Series, and Products*,7th ed. San Diego, CA, Elsevier Inc, 2007.

[9] A. P. Prudnikov, Yu. A. Brychkov, and O. I. Marichev, Integrals and series. Vol. 3, Gordon and Breach Science Publishers, New York, 1990. More special functions; Translated from the Russian by G. G. Gould. MR 1054647 (91c:33001)

[10] Y. Rahmatallah and S. Mohan, "Peak-To-Average Power Ratio Reduction in OFDM Systems: A Survey And Taxonomy," in IEEE Communications Surveys & Tutorials, vol. 15, no. 4, pp. 1567-1592, Fourth Quarter 2013.

[11] "The Wolfram functions site for special mathematical functions." Wolfram Research, Inc 2017. Available: http://functions.wolfram.com